Journal of Applied Electrochemistry (2005) 35:757–763
DOI 10.1007/s10800-005-1365-9

Enhanced photocatalytic degradation of tetramethylammonium on silica-loaded titania

MUHAMMAD SHARIQ VOHRA[1,2], JAESANG LEE[1] and WONYONG CHOI[1,*]
[1]*School of Environmental Science and Engineering, Pohang University of Science and Technology, Pohang, 790-784, Korea;* [2]*Present Address: Civil Engineering Department, King Fahd University of Petroleum and Minerals, Dhahran, Kingdom of Saudi Arabia 31261*
*(*author for correspondence, e-mail: wchoi@postech.ac.kr)*

Received 15 June 2004; accepted in revised form 15 November 2004

Key words: photocatalytic oxidation, surface modification, TiO_2, SiO_2, water treatment

Abstract

Photocatalytic degradation (PCD) of tetramethylammonium (TMA) in water was studied using both pure TiO_2 and silica-loaded TiO_2 (Si–TiO_2). Use of Si–TiO_2 catalyst prepared from commercial TiO_2 powder by a simple method developed in this work enhanced the PCD rate of TMA considerably. The Si/Ti atomic ratio of 18% was found to be an optimum in photoactivity and the calcined sample was more efficient than the uncalcined one. Several factors were noted to be responsible for the higher photoefficiency of Si–TiO_2 catalyst. Si–TiO_2 calcined at 700 °C did not show any sign of change in the crystalline structure from that of uncalcined pure TiO_2. The increased thermal stability of Si–TiO_2 enabled the bulk defects to be removed at high temperatures without forming the inactive rutile phase, which may partly contribute to the higher photoactivity. The most outstanding characteristics of Si–TiO_2 is its surface charge modification. Loading silica on to a titania surface made the surface charge highly negative, which was confirmed by zeta potential measurements. The enhanced electrostatic attraction of cationic TMA onto the negatively charged Si–TiO_2 surface seems to be the main reason for the enhanced photoactivity of Si–TiO_2. As a result of this surface charge change, the TMA PCD rate with Si–TiO_2 exhibited a maximum around pH 7 whereas the PCD with pure TiO_2 was minimized at pH 7. The X-ray photoelectron spectroscopic analysis showed the formation of SiO_x on the TiO_2 surface but the diffuse reflectance UV spectra indicated no significant difference in the band gap transition between pure TiO_2 and Si–TiO_2. In addition, the diffuse reflectance IR spectra showed the presence of more surface OH groups on Si–TiO_2 than on pure TiO_2, which may also contribute to the higher photoactivity of Si–TiO_2 through generating more OH radicals upon UV illumination.

1. Introduction

Semiconductor photocatalysis is based on photoinduced surface chemical redox reactions and the role of the surface is critical in determining the reaction kinetics, mechanisms, and products. TiO_2 has been most intensively studied as a successful photocatalyst for the photocatalytic degradation (PCD) of various pollutants and its surface has been modified in various ways such as platinum deposition [1–4], inorganic oxide loading [5–7], sensitizer anchoring [8, 9], surfactant or polymer coating [10–13] and fluorination [14–17]. The surface modifications can promote the adsorption of some pollutants through changing the surface charge characteristics of TiO_2 or can enhance the charge separation efficiency by providing electron/hole trap sites to accelerate the mineralization rates. Silica-loaded TiO_2 (Si–TiO_2) has been reported to enhance the PCD rates of organic pollutants such as cetylpyridinium bromide [18] and rhodamine 6G [6, 19]; this effect was attributed to the enhanced electrostatic attraction between the anionic Si–TiO_2 surface and the cationic substrate molecules. On the other hand, Jung and Park [20] reported that PCD of trichloroethylene, a neutral substrate, was also accelerated on Si–TiO_2 and ascribed this to the enhanced surface OH group density and reduced bulk defects. The addition of silica to titania prevented the agglomeration of nano-sized anatase particles while producing higher surface area and higher photoreactivity for phenol degradation [21]. In a similar context, Si–TiO_2 showed better photoactivity for degrading ethylene [5] and cyanide [22]. In addition, the presence of silica in TiO_2 significantly inhibited the thermal phase transition from anatase to rutile even at 1000 °C, whereas the phase transition to rutile in pure TiO_2 was noted at 625 °C and completed at 1000 °C [7].

In this work, we prepared Si–TiO_2 using our own method and characterized it as a highly active photocatalyst for degrading cationic substrates. Tetratmethylammonium ($(CH_3)_4N^+$ or TMA) was chosen as a model substrate because of its widespread use in the electronics industry as a silicon etchant. As TMA is very stable and non-biodegradable, conventional wastewater treatment technology is not efficient in degrading it. Kim and Choi [23] demonstrated that TMA can be successfully degraded in UV-illuminated TiO_2 suspensions but the degradation rate was slow: 90% degradation of 0.1 mM TMA required about 6 h UV irradiation. The development of better photocatalysts is needed to use PCD to control TMA in wastewaters. The Si–TiO_2 photocatalyst prepared in this work exhibited much higher reactivity for TMA degradation than pure TiO_2. Several experimental parameters that may explain the enhanced efficiency of Si–TiO_2 were investigated. In addition, the Si–TiO_2 catalyst was synthesized through a simpler method than following the previously reported sol–gel methods.

2. Experimental

2.1. *Reagents and materials*

The following reagent-grade chemicals were used as received: Si $(OC_2H_5)_4$ (Aldrich), TiO_2 (Degussa P25), $(CH_3)_4$ NCl (ACROS Organics), $(CH_3)_3$ NHCl (Aldrich), $(CH_3)_2NH_2Cl$ (Sigma), CH_3 NH_3Cl (Sigma), NH_4Cl (Aldrich), $(C_2H_5)_4NCl$ (Sigma), methanesulfonic acid (Aldrich), Na_2 CO_3 (S.P.C. GR Reagent, Japan), $NaHCO_3$ (Kanto, Japan), CH_3CN (Aldrich), HCl (S.P.C. GR Reagent, Japan), and NaOH (S.P.C. GR Reagent, Japan). A Barnstead water purification setup was employed to obtain the deionized water (18 MΩ cm).

2.2. *Silica–TiO $_2$ Si–TiO $_2$ synthesis*

The Si–TiO_2 catalyst samples were synthesized as follows. An aliquot of $Si(OC_2H_5)_4$ (tetraethylorthosilicate: TEOS) liquid was directly added to the commercial TiO_2 powder (P25) with a gradual mixing to ensure its uniform coating on the TiO_2 particles. The mixing ratios of Si/Ti were varied to find an optimal composition. The mixed sample was left overnight for drying and then calcined at 700 °C for 5 h. The calcined samples were used without further treatment.

2.3. *Photocatalytic degradation reactions*

All the PCD experiments were carried out using a Pyrex reactor (33 ml) with a quartz window. The catalyst powder was well suspended at 0.5 g l^{-1} in 27 ml deionized water by sonicating for 30 s. An aliquot of 3 ml from 1 mM TMA stock solution was then added to obtain $[(CH_3)_4N^+]_0$ = 100 μM. The PCD of tetraethylammonium ($(C_2H_5)_4N^+$ or TEA) was also carried out for comparison. The initial pH (pH_i) of the suspension was adjusted with HCl or NaOH standard solutions. A Xe-arc lamp (300 or 450 W, Oriel) was used as the illumination source and the incident light was filtered through a 10-cm IR water filter and a UV-cutoff (λ > 300 nm) filter. The incident light intensity in the active wavelength region (300–400 nm) was estimated to be around 1×10^{-4} Einstein min^{-1} l^{-1} using ferrioxalate actinometry [24]. Sample aliquots of 1 ml were collected at appropriate time intervals and filtered through 0.45-μm PTFE filters (Millipore). The reactor was kept sealed using a rubber septum throughout the illumination period.

2.4. *Analysis and catalyst characterization*

TMA and its degradation products/intermediates were analyzed using a Dionex ion chromatograph (IC, DX-120) equipped with a conductivity detector, and Dionex Ionpac column CS-14 (4 mm × 250 mm; CG-14 Guard, 4 mm × 50 mm) for cation analysis and AS-14 (4 mm × 250 mm; AG-14 Guard, 4 mm × 50 mm) for anion analysis. The eluent compositions were 10 mM methanesulfonic acid for the cation analysis, and 3.5 mM Na_2CO_3/1 mM $NaHCO_3$ for the anion analysis. For TEA analysis, the eluent composition was 8 mM methanesulfonic acid with 10% CH_3CN.

The optical absorption spectra of pure TiO_2 and Si–TiO_2 powders were recorded using a Shimadzu UV–Vis spectrophotometer equipped with a diffuse reflectance attachment (Shimadzu ISR-2200). All sample powders were diluted with $BaSO_4$ (TiO_2:$BaSO_4$ = 1:17) and referenced to $BaSO_4$. The diffuse reflectance infrared Fourier transform spectra (DRIFTS) were obtained using a Bomem DA3-FTIR spectrometer containing a diffuse reflectance accessory of Harrick (model DRA-2CE) and a triglycine sulfate detector (DTGS). The surface atomic compositions of Si–TiO_2 catalysts were determined by X-ray photoelectron spectroscopy (XPS: Kratos XSAM 800 pci) using MgKα line (1253.6 eV) as an excitation source. The spectra were taken for each sample after Ar^+ (3 keV) sputter cleaning. The binding energies (BE) of all peaks were referenced to the Ti 2p line (458.8 eV) in TiO_2 and checked against C 1s line (284.6 eV) originating from surface impurity carbons. The crystalline phase contents of pure TiO_2 and Si–TiO_2 were analyzed using X-ray powder diffraction (XRD: Rigaku Model D/Max III) with CuKα radiation. The electrophoretic mobilities of TiO_2 and Si–TiO_2 particles suspended in water were measured to determine their zeta potentials as a function of pH by using an electrophoretic light scattering spectrophotometer (ELS 8000, Otsuka) equipped with a He–Ne laser and a thermostated flat board cell.

3. Results and discussion

3.1. *Enhanced PCD of TMA with Si–TiO_2*

Figure 1 compares the distribution of products and intermediates generated as a result of TMA PCD in the

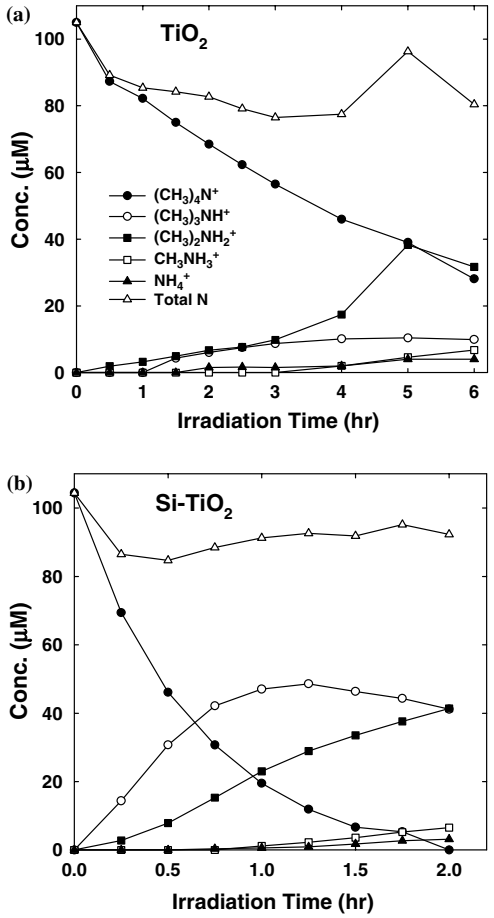

Fig. 1. Products and intermediates generated during the photocatalytic degradation of TMA: (a) pure TiO_2, (b) Si–TiO_2 (with 18% Si/Ti) calcined at 700 °C. $[TMA]_o$ = 100μM, [Catalyst] = 0.5 g L^{-1}, pH_i = 5.

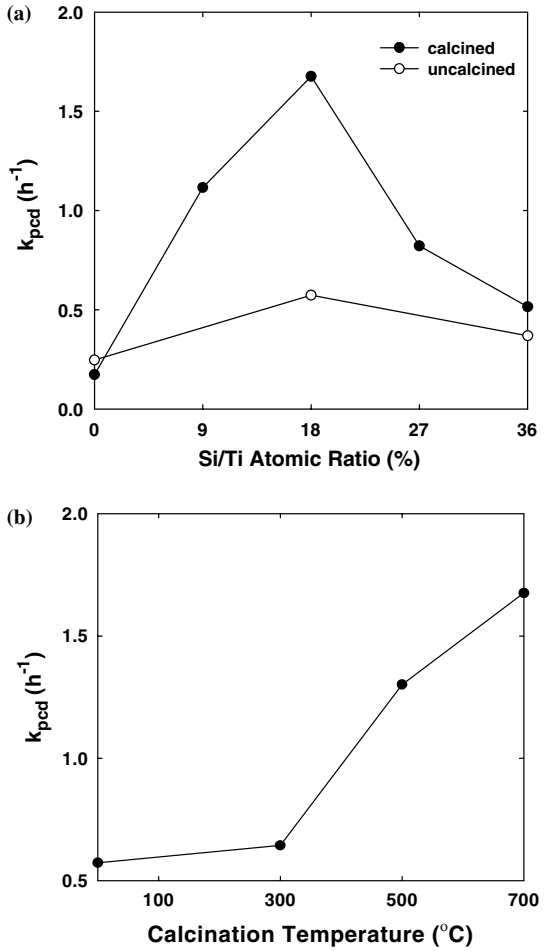

Fig. 2. TMA photocatalytic degradation rate constant (k_{pcd} for the initial 1 h) as a function of (a) the Si/Ti atomic ratio (%) and (b) the calcination temperature (with Si–TiO_2 of 18% Si/Ti). $[TMA]_o$ = 100 μM, [Catalyst] = 0.5 g L^{-1}, pH_i = 5.

UV-illuminated suspensions of pure TiO_2 and Si–TiO_2. The main N-containing products are $(CH_3)_3NH^+$, $(CH_3)_2NH_2^+$, $(CH_3)NH_3^+$, and NH_4^+, which is consistent with the previous observation [23] that TMA PCD on pure TiO_2 proceeded through successive demethylation steps producing NH_4^+ in acidic pH and NO_2^- /NO_3^- in alkaline pH as a final product. With longer PCD time, NO_2^- and NO_3^- may also result in the present systems. Hundred percentage conversion of TMA was achieved in 2 h with Si–TiO_2 whereas less than 80% conversion was obtained even after 6 h with pure TiO_2. The intermediate distribution in Si–TiO_2 suspension is different from that in TiO_2 suspension. In particular, the production of $(CH_3)_3NH^+$ was markedly enhanced with Si–TiO_2, which is not clearly understood. Silica loading on TiO_2 surface changes not only the kinetics but also the mechanism of TMA PCD.

Figure 2(a) compares the PCD rate constants (k_{pcd}) of TMA as a function of Si content between the uncalcined and calcined Si–TiO_2 samples and Figure 2(b) shows the variation of k_{pcd} as a function of the calcination temperature. Both uncalcined and calcined samples show an optimal photoactivity with 18% Si/Ti atomic ratio at which the calcination-induced photoactivity enhancement is the largest. The reduced photoactivity with higher Si content is probably due to the complete coverage of the TiO_2 surface with silica. The Si–TiO_2 sample with 18% Si/Ti was then calcined at several different temperatures: the PCD rate increased with increasing calcination temperature up to 700 °C, as shown in Figure 2(b). All other experiments in this work were thus conducted using the Si–TiO_2 (18% Si/Ti) catalyst calcined at 700 °C.

3.2. *Factors contributing to the higher photoactivity of Si–TiO_2*

Various factors which account for the enhanced photoactivity of Si–TiO_2 may include the surface chemical composition, specific surface area, crystallinity, surface charge characteristics, band gap energy, surface hydroxyl group density, defect sites, etc. All of these parameters may affect the interactions taking place between the substrate molecules and the catalyst surface. Some of these parameters were discussed below to understand the enhanced photoactivity of Si–TiO_2.

The surface atomic ratios of Si/Ti in Si–TiO_2 samples, which were obtained from the XPS analysis, were determined to be 0.29 with 4% Si/Ti sample; 0.50 with 11% Si/Ti sample; 0.96 with 18% Si/Ti sample; 2.08 with 36% Si/Ti sample. It is interesting to note that the Si–TiO_2 catalyst with the optimal Si content (18% Si/Ti) has a near one-to-one ratio of Si/Ti in the surface region. The XPS spectra of Si–TiO_2 in Figure 3 show that the BE of Si 2p electrons gradually increases from 102.5 to 103.1 eV with increasing the Si/Ti ratio from 4 to 36%. That is, as the Si content increases, the Si BE approaches that of bulk SiO_2 (103.35 eV). This indicates that the fraction of Si–O–Ti linkages decreases but that of Si–O–Si linkages increases with increasing the Si content in Si–TiO_2 [25].

The XRD spectra of the calcined pure TiO_2, pure TiO_2 (P25), and calcined Si–TiO_2 samples are compared in Figure 4. The anatase to rutile ratio in Si–TiO_2 (calcined at 700 °C) was the same as that of uncalcined TiO_2 (80:20), whereas the rutile content in calcined TiO_2 was highly enhanced. The presence of Si in TiO_2 enhanced the thermal stability of the catalyst and inhibited the phase transformation to rutile even up to 700 °C, which is consistent with previous work of Jung and Park [20]. Typical pure TiO_2 samples undergo phase transformation from the anatase to rutile at a temperature as low as 625 °C [5, 7]. The fact that the XRD spectrum of Si–TiO_2 calcined at 700 °C is identical to that of uncalcined TiO_2 implies that the crystallite phase and size are not responsible for the higher reactivity of Si–TiO_2. Calcining Si–TiO_2 should reduce the bulk defects that decrease the photoactivity. On the other hand, the phase transition to rutile, which typically accompanies the high temperature calcination and decreases the photoactivity, is inhibited with Si–TiO_2 because of its increased thermal stability. The calcination effect on the photoactivity of Si–TiO_2 seems to be patially related to reducing defect sites.

A higher adsorption of substrates enhances the PCD rate. Tada et al. [18] reported that both the adsorption of cetylpyridinium bromide and its PCD rate were markedly enhanced on Si–TiO_2 (at pH 5–6) as compared to pure TiO_2. Anderson and Bard [6] have also suggested that the adsorption of R-6G on SiO_2 sites lead to increased PCD rate. However, TMA was not significantly adsorbed on both pure TiO_2 and Si–TiO_2. Negligible TMA adsorption on TiO_2 in the pH range 3–9 was also reported previously [16]. Different from TMA, a notable amount of tetraethylammonium (TEA) was adsorbed on both pure TiO_2 and Si–TiO_2 (compare the concentrations at time zero in Figure 5). However, the initial substrate adsorption was nearly the same for both catalysts and hence does not explain the highly enhanced PCD of TEA on Si–TiO_2, shown in Figure 5. Nevertheless, it is interesting to note that the PCD rates of TEA are much higher than those of TMA for both pure TiO_2 and Si–TiO_2 (compare Figures 1 and 5), which might be ascribed to the higher initial adsorption of TEA on the catalyst surface. It is speculated that the

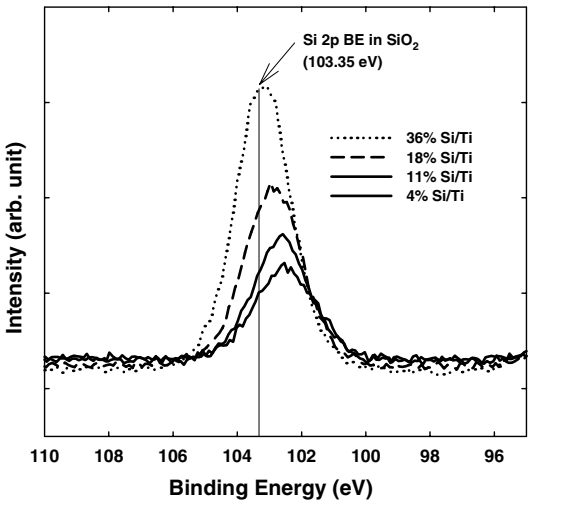

Fig. 3. The XPS spectra of Si (2p band) on TiO_2 that was loaded with varying amounts of Si.

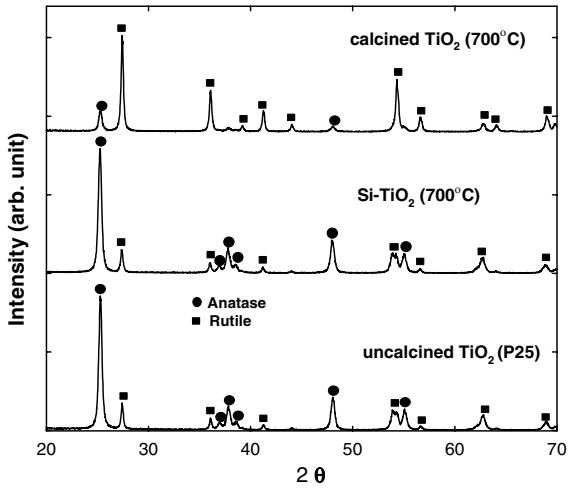

Fig. 4. The XRD spectra of pure TiO_2, Si–TiO_2 (18% Si/Ti) calcined at 700 °C, and pure TiO_2 calcined at 700 °C.

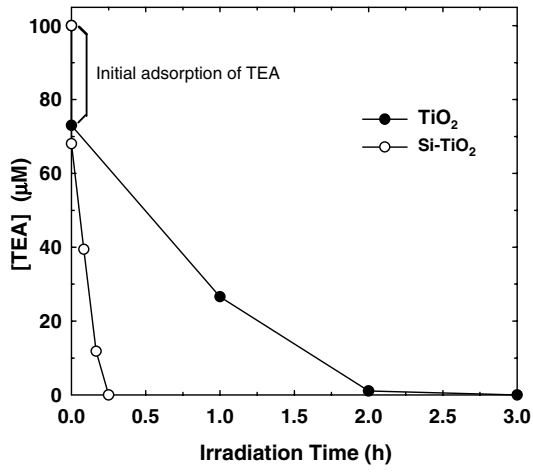

Fig. 5. TEA photocatalytic degradation using the pure TiO_2 and Si–TiO_2 (18% Si/Ti sample calcined at 700 °C). $[TEA]_o$ = 100 μM, [Catalyst] = 0.5 g L^{-1}, pH_i = 5.

enhanced hydrophobic interactions between the ethyl groups and catalyst surface are responsible for the higher adsorption of TEA. On the other hand, the specific surface area (SSA) is another important parameter that determines the photoactivity of catalysts. Photocatalysts with higher SSA may exhibit higher PCD rates because more substrate-adsorption sites are available. For example, Vohra and Tanaka [26] demonstrated that the increase in PCD rate of paraquat on Si–TiO_2 resulted from the larger SSA induced by a higher Si content. In this study, the SSA values of pure TiO_2 and Si–TiO_2 were found to be similar (52 and 55 $m^2\ g^{-1}$, respectively) and hence do not explain for the large enhancement in the PCD rate with Si–TiO_2.

The surface charge characteristics should also be considered. The surface charge on TiO_2 in pure water results from the pH-dependent speciation of surface hydroxyl groups, which is described by the following reactions.

$$\equiv \mathrm{Ti{-}OH_2^+} \leftrightarrow \equiv \mathrm{Ti{-}OH} + \mathrm{H^+} \quad (1)$$

$$\equiv \mathrm{Ti{-}OH} \leftrightarrow \equiv \mathrm{Ti{-}O^-} + \mathrm{H^+} \quad (2)$$

As for the P25 TiO_2 (as used in this study), a pH_{zpc} (zero point of charge) value of 6.5 has been reported [27]. Therefore, the TiO_2 surface is negatively charged at pH > 6.5 and positively charged at pH < 6.5. According to a simple electrostatic model, TMA should be more attracted onto the TiO_2 surface at alkaline pH, which has been previously confirmed by measuring the attenuated total reflection FTIR (ATR–FTIR) spectra of the interface of TiO_2/TMA solution [23]. Although TMA does not adsorb on the TiO_2 surface, its concentration seems to be enhanced near the surface region of TiO_2 at alkaline pH. The deposition of silica on TiO_2 is expected to change the surface charge characteristics significantly since the pH_{zpc} of SiO_2 is about 2. Previous studies have reported that the pH_{zpc} of Si–TiO_2 is much lower than that of pure TiO_2 [28, 29]. Figure 6 shows the change in zeta potentials of pure TiO_2 and Si–TiO_2 particles suspended in water as a function of pH. The point of zero zeta potential (PZZP) of TiO_2, which is practically equivalent to pH_{zpc}, is about 6.5, which agrees with the literature value. Note that the PZZP of Si–TiO_2 is significantly shifted to lower pH and that the surface charge of Si–TiO_2 is more negative than that of pure TiO_2 over the whole pH range. Therefore, cationic TMA should be more favorably attracted onto the Si–TiO_2 surface electrostatically. In agreement with this electrostatic consideration, Figure 7 shows that the TMA PCD rates with Si–TiO_2 are consistently higher than those with pure TiO_2 at most pH. With Si–TiO_2, increasing pH accompanies the increase in negative charge density (see Figure 6) and hence higher concentrations of TMA near the surface region. Accordingly, the TMA PCD on Si–TiO_2 increased with pH (< 7). At pH 3, however, Si–TiO_2 did not show a higher reactivity than pure TiO_2 although the surface charge condition of Si–TiO_2 is more favorable for attracting TMA than that of pure TiO_2. This seems to be due to the fact that suspended Si–TiO_2 particles are agglomerated at pH 3, near the PZZP of Si–TiO_2 (see Figure 6), whereas pure TiO_2 particles should be well suspended at pH 3. Similarly, the reactivity of pure TiO_2 was minimized around pH 7 (near PZZP of pure TiO_2) because of agglomeration, while Si–TiO_2 particles, in contrast should be well dispersed at this pH. The negative charge density on Si–TiO_2 surface seems to be saturated above pH 7 but the PCD rate decreased with increasing pH 7 to 9. This appears to be due to a higher ionic strength at pH 9 which induces agglomeration of Si–TiO_2 particles. Loading silica onto TiO_2 significantly increased the

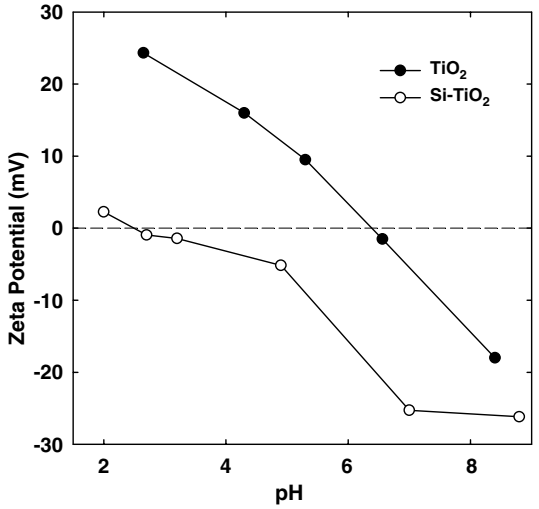

Fig. 6. Zeta potentials of TiO_2 and Si–TiO_2 particles in aqueous suspensions ([TiO_2] = [Si–TiO_2] = 2 mg L^{-1}) as a function of pH.

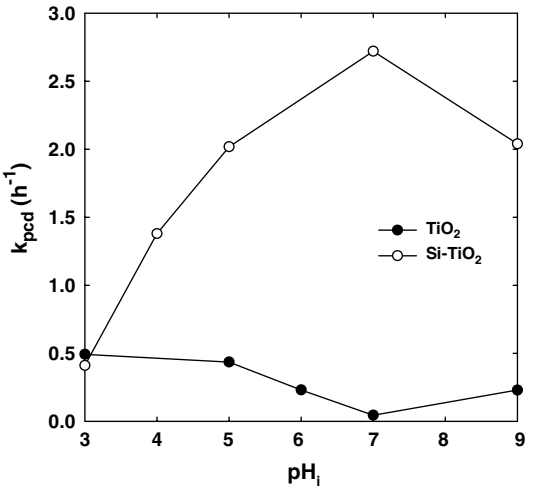

Fig. 7. TMA photocatalytic degradation rate constant (k_{pcd} for the initial 1 h) as a function of the initial pH (pH_i) with Si–TiO_2 (18% Si/Ti sample calcined at 700 °C) and pure TiO_2. $[TMA]_o$ = 100 μM, [Catalyst] = 0.5 g L^{-1} (a 300 W lamp was used in this experiment whereas a 450 W lamp was used in all other cases).

negative surface charge density and hence increased the PCD rate of cationic TMA. Conversely, the modification of the TiO_2 surface with a MgO_X monolayer, which shifted the pH_{zpc} from 7.5 to 8.7 with increasing positive surface charge density, enhanced the PCD rate of an anionic substrate (dodecylbenzenesulfonate) at pH 7 [30].

The loading of silica on TiO_2 may have an influence on the band gap transition. For example, a significant blue shift of absorption edge in the diffuse reflectance UV spectra of Si–TiO_2 samples was observed with increasing Si content [31]. However, Figure 8(a) shows that there is little difference in the band gap transition between pure TiO_2 and Si–TiO_2 synthesized in this work. The enhanced reactivity of Si–TiO_2 cannot be ascribed to enhanced UV absorption. Another factor that may contribute to the activity of photocatalysts is the surface hydroxyl group density. It has been previously reported that Si–TiO_2 had much higher surface OH groups as compared to pure TiO_2, which contributed to the increased photoactivity of Si–TiO_2 [20]. Figure 8(b) compares the DRIFT spectra of pure TiO_2 and Si–TiO_2. It is evident that the Si–TiO_2 has a higher O-H stretching intensity (centered around 3400 cm^{-1}) and should have more surface OH groups than pure TiO_2. Since the surface OH group is the precursor of the photoinduced OH radical formation and the TMA PCD should be initiated by an OH radical attack [23], a higher surface OH group density may contribute to a higher PCD rate as observed in this work.

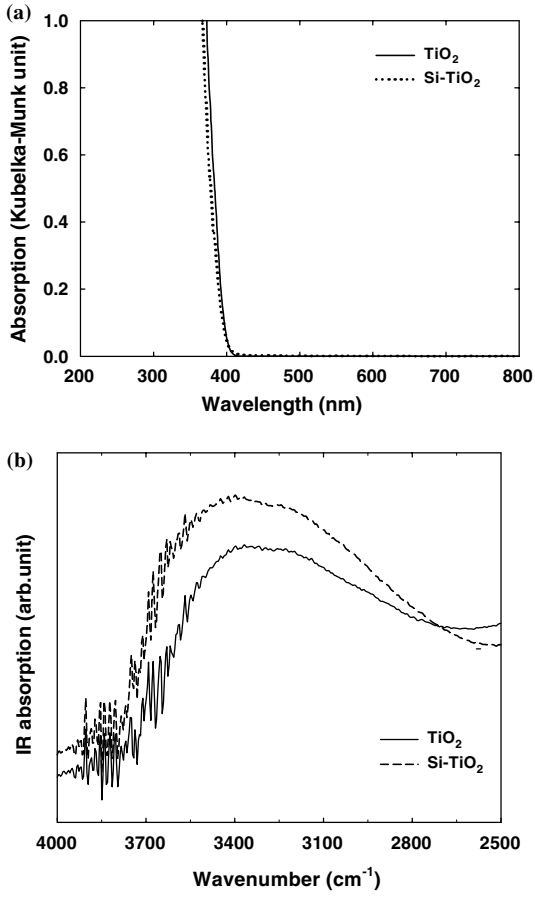

Fig. 8. (a) The UV–Visible diffuse reflectance spectra and (b) the DRIFTS spectra of pure TiO_2 and Si–TiO_2 (18% Si/Ti calcined at 700 °C) powder samples.

4. Conclusions

A significantly enhanced PCD of TMA could be achieved using a Si–TiO_2 catalyst, which was synthesized using a very simple method. Silica was loaded on the surface of commercial TiO_2 particles by simple mixing with TEOS. For both calcined and uncalcined Si–TiO_2 samples, a Si/Ti atomic ratio of 18% was found to be an optimum in photoactivity and the calcined sample was more efficient than the uncalcined one. Loading of silica on the titania surface made the surface charge highly negative. The stronger electrostatic attraction of cationic TMA onto the negatively charged Si–TiO_2 surface seems to be the main reason for the enhanced photoactivity of Si–TiO_2. The present work proposes a simple method to synthesize highly photoactive Si–TiO_2 catalyst for the efficient removal of TMA and other cationic pollutants from wastewaters.

Acknowledgement

We gratefully acknowledge supports provided by KOSEF through the Center for Integrated Molecular Systems (CIMS) and by the Brain Korea 21 project.

References

1. B. Kraeutler and A.J. Bard, *J. Am. Chem. Soc.* **100** (1978) 4317.
2. J. Lee, H. Park and W. Choi, *Environ. Sci. Technol.* **36** (2002) 5462.
3. S. Kim and W. Choi, *J. Phys. Chem. B* **106** (2002) 13311.
4. W. Choi, J. Lee, S. Kim, S. Hwang, M.C. Lee and T.K. Lee, *J. Ind. Eng. Chem.* **9** (2003) 96.
5. X. Fu, L.A. Clark, Q. Yang and M.A. Anderson, *Environ. Sci. Technol.* **30** (1996) 647.
6. C. Anderson and A.J. Bard, *J. Phys. Chem.* **99** (1995) 9882.
7. C. Anderson and A.J. Bard, *J. Phys. Chem.* **101** (1997) 2611.
8. Y. Cho, W. Choi, C.-H. Lee, T. Hyeon and H.-I. Lee, *Environ. Sci. Technol.* **35** (2001) 966.
9. E. Bae and W. Choi, *Environ. Sci. Technol.* **37** (2003) 147.
10. M.S. Vohra and K. Tanaka, *Environ. Sci. Technol.* **35** (2001) 411.
11. H. Tada, H. Matsui, F. Shiota, M. Nomura, S. Ito, M. Yoshihara and K. Esumi, *Chem. Commun.* (2002) 1678.
12. Q. Huang and C.-S. Hong, *Chemosphere* **41** (2000) 871.
13. Y. Cho, H. Kyung and W. Choi, *Appl. Catal. B Environ.* **52** (2004) 23.
14. C. Minero, G. Mariella, V. Maurino and E. Pelizzetti, *Langmuir* **16** (2000) 2632.
15. C. Minero, G. Mariella, V. Maurino, D. Vione and E. Pelizzetti, *Langmuir* **16** (2000) 8964.
16. M.S. Vohra, S. Kim and W. Choi, *J. Photochem. Photobiol. A Chem.* **160** (2003) 55.
17. H. Park and W. Choi, *J. Phys. Chem. B* **108** (2004) 4086.

18. H. Tada, Y. Kubo, M. Akazawa and S. Ito, *Langmuir* **14** (1998) 2936.
19. H. Tada, M. Akazawa, Y. Kubo and S. Ito, *J. Phys. Chem. B* **102** (1998) 6360.
20. K.Y. Jung and S.B. Park, *Korean J. Chem. Eng.* **18** (2001) 879.
21. Z. Ding, G.Q. Lu and P.F. Greenfield, *J. Colloid Interface Sci.* **232** (2000) 1.
22. M.S. Ahmed and Y.A. Attia, *J. Non-Cryst. Solids* **186** (1995) 402.
23. S. Kim and W. Choi, *Environ. Sci. Technol.* **36** (2002) 2019.
24. C.G. Hatchard and C.A. Parker, *Proc. R. Soc. London, Ser. A* **235** (1956) 518.
25. H. Tada, *Langmuir* **12** (1996) 966.
26. M.S. Vohra and K. Tanaka, *Water Res.* **37** (2003) 3992.
27. A.T. Stone, A. Torrents, J. Smolen, D. Vasudevan and J. Hadley, *Environ. Sci. Technol.* **27** (1993) 895.
28. Y.-L. Lin, T.-J. Wang and Y. Jin, *Powder Technol.* **123** (2002) 194.
29. H. Chun, W. Yizhong and T. Hongxiao, *Appl. Catal. B Environ.* **35** (2001) 95.
30. H. Tada, M. Yamamoto and S. Ito, *Langmuir* **15** (1999) 3699.
31. Z. Liu and R.J. Davis, *J. Phys. Chem.* **98** (1994) 1253.